

Effect of Anion Polarization on Conductivity Behavior of Poly(ethylene oxide) Complexed with Alkali Salts

S. Besner, A. Vallée, G. Bouchard, and J. Prud'homme*

Department of Chemistry, University of Montreal, Montreal, Quebec, Canada H3C 3J7

Received June 9, 1992; Revised Manuscript Received August 19, 1992

ABSTRACT: Conductivity behavior of poly(ethylene oxide) (PEO) amorphous electrolytes containing MCF_3SO_3 ($\text{M} = \text{Li, K, Rb, or Cs}$) in a molar ratio $\text{EO/M} = 9$ agrees with anterior data reported on PEO-MSCN ($\text{M} = \text{Li, K, or Cs}$) amorphous electrolytes. At any reduced temperature $T - T_g$ (T_g = glass transition temperature) over the range $30 < T < 100^\circ\text{C}$ of the study, ionic conductivity increases in the same ratio as the square of the cation radius. This correlation, which suggests a strong coupling between the internal mobilities of the ions of opposite charge, was previously interpreted in terms of cation-oxygen binding energy. However, a complementary study made on PEO amorphous electrolytes containing a series of lithium salts, including LiB(Ph)_4 , LiClO_4 , and $\text{LiN(CF}_3\text{SO}_2)_2$ in addition to LiCF_3SO_3 and LiSCN , shows that conductivity decreases with increasing anion polarizability. By analogy with molten salt mixtures, this latter feature is attributed to a polarization of the anions due to the asymmetry in the local distribution of the solvated cations. Since polarizing power of alkali cations decreases with increasing cation size, it is likely that this effect, which is noticeable for both LiCF_3SO_3 and LiSCN , plays a part in the correlation between conductivity and cation size.

Introduction

Poly(ethylene oxide) (PEO) and other polyethers can form ionic complexes with metal salts of low lattice energy.¹ Among these complexes, those with lithium salts are the most studied because of their potential application as solvent-free, solid electrolytes in lithium rechargeable batteries.² In their optimal form, these electrolytes are rubbery materials that involve liquidlike molecular motion at the microscopic level. They may be considered as the polymeric counterpart of the aprotic, liquid electrolytes currently used in primary lithium batteries.^{3,4} Their ionic conductivity (σ) exhibits a broad maximum over the concentration range $c = 0.3\text{--}2\text{ mol/kg}$ in the concentrated regime.^{1,2} As shown by Armand et al.,⁵ at a given concentration over this range, the temperature dependence of σ can be fitted to the same phenomenological equation as that proposed by Angell⁶ for molten salts and fused hydrates. This equation, which may be derived from the Vogel-Tammann-Fulcher (VTF) equation for fluidity of glass-forming liquids,⁷ is

$$\sigma(T) = A \exp[-B/(T - T_0)] \quad (1)$$

where A and B are empirical factors, and T_0 is the ideal glass transition temperature, a quantity systematically inferior to the value of T_g measured by DSC.

Although eq 1 provides a reliable basis to interpret ion transport in terms of general concepts, such as free volume and configurational entropy,^{1,7} it does not give any information on the molecular, local features that govern the conduction process. At the upper range of the concentration domain, the physical situation in polymer electrolytes approaches that in molten salts. The total energy of the system should be minimum when each ion is surrounded by ions of opposite charge. Therefore, any factor susceptible to perturb the local symmetry may have a great effect on the dynamics of the individual ions. In the case of molten salts, an example of this feature is found in the conductivity behavior of monovalent, binary salt mixtures (i.e., pairs of salts with a common anion). In these mixtures,⁷ a polarization of the anions due to the asymmetry of the cationic environment yields substantial changes in the self-diffusion coefficients and internal

mobilities of the ions with respect to those of the pure components.

Recent work on ion dynamics in concentrated electrolytes made with ethylene oxide oligomers reveals interesting features that suggest that anion polarization may play a part in the conduction process of polymer electrolytes. As reported in an NMR study of LiCF_3SO_3 by Boden et al.⁸ and in a radiotracer study of NaSCN by Al-Mударis and Chadwick,⁹ the self-diffusion coefficients of the ions of opposite charge appear to be nearly identical in these electrolytes. Furthermore, at moderate temperatures their conductivity magnitudes were reported to be comparable to the values of σ computed from the self-diffusion data by assuming a complete dissociation of the salts. This feature indicates that a strong coupling occurs between the internal mobilities of ions of opposite charge. Since asymmetry in ion distribution necessarily arises from the irregular geometry of the cation solvation shells, such a coupling, which results from ion-ion interactions, may involve a specific effect due to anion polarization.

Evidence for a strong coupling between anion and cation mobilities may be also found in the effect of cation size on the conductivity magnitude of PEO concentrated electrolytes. As reported in a former work,¹⁰ in their amorphous (or melted) state, such electrolytes containing LiSCN , KSCN , and CsSCN in a molar ratio $\text{EO/salt} = 8\text{--}9$ exhibit conductivity magnitudes at the same reduced temperatures $T - T_0$ that increase in the same ratio as the cation surface (or the square of the cation radius). This feature was interpreted as an indication that ion mobility increases in the same ratio as the inverse of the cation-oxygen binding energy. It was then argued that, for a given anion under a corresponding state of segmental motion (or thermal energy), ion mobility is mostly governed by the rate of cation jumps through the coordination sites. Such a comparison based on a series of salts with a common anion did not allow the separation of the effect of ion-ion interactions from that of the ion-polymer interactions. It was thus assumed that the ion-ion interactions were the same in the different electrolytes.

In the present work, an attempt is made to elucidate the role of the ion-ion interactions by studying the effect of the nature of the anion on the conductivity magnitude of PEO electrolytes of high salt contents. The first part

Table I
Molecular Weights (M_n) and Weight Fractions (W_x) of the Oligomers HO-(CH₂CH₂O)_x-H in the PEG200 Sample Used for Preparing Copolymer P(OM/PEG200)^a

x	M_n (g mol ⁻¹)	W_x (%)
3	150	3.9
4	194	45.4
5	238	24.1
6	282	16.5
7	326	6.0
8	370	4.1

^a $M_n = 223$; $M_w/M_n = 1.04$.

of this work is devoted to the conductivity behavior of a second series of alkali salts with a common anion. The study of these salts, which share the triflate anion, provides further evidence for a strong coupling between cation and anion mobilities. The phase diagrams constructed for the corresponding systems show that amorphous electrolytes with a high salt content (EO/salt = 9) can be obtained at moderate temperatures ($30 < T < 100$ °C) with KCF₃SO₃, RbCF₃SO₃, and CsCF₃SO₃ but not with LiCF₃SO₃ and NaCF₃SO₃. To extend the study to a wider range of cation sizes, attempts were made to prepare amorphous electrolytes of the same composition by using oxymethylene-linked PEO copolymers similar to those described by Booth et al.¹¹ These attempts were successful in the case of LiCF₃SO₃ only. Surprisingly, even under their optimal form, that is, with very short, nonuniform, and noncrystallizable oligomeric PEO segments, these copolymers did form crystalline compounds with both NaCF₃SO₃ and KCF₃SO₃.

The second part of this work is devoted to the conductivity behavior of a series of lithium salts with anions of different polarizability (or softness). The data provide evidence for a correlation between the conductivity magnitude and the anion polarizability. The salts, which include LiB(Ph)₄, LiSCN, LiClO₄, and LiN(CF₃SO₂)₂, were examined in a molar ratio EO/Li = 11. This composition was imposed by the features in the phase diagram of the PEO-LiB(Ph)₄ system. It corresponds to the highest salt content that yields homogeneous, amorphous electrolytes over the range above 50 °C. Also presented are arguments based on the conductivity behavior of the same salts in ether solvents that reinforce the view that a substantial ionic dissociation takes place in concentrated PEO electrolytes.

Experimental Section

Materials. The detail concerning the purification and the characterization of the PEO sample ($M_n = 3.9 \times 10^3$, $M_w/M_n = 1.02$) was reported in a previous work.¹⁰ The oxymethylene-linked PEO sample was prepared according to the polycondensation reaction described by Booth et al.,¹¹ that is, a Williamson reaction between a low molecular weight poly(ethylene glycol) (PEG) and dichloromethane in presence of an excess of KOH. For that purpose, PEG200 described in Table I (25 g) was added in the dark, under dry nitrogen, to a mixture of KOH (25 g) and CH₂Cl₂ (100 mL). After 16 h of reaction at room temperature, the mixture (a slurry) was diluted with CH₂Cl₂ (600 mL) and filtered on Celite. The resulting, clear solution was then washed with deionized water, dried over molecular sieves, and evaporated under vacuum. The product of this reaction (23 g, $M_{GPC} = 8 \times 10^3$) was dissolved in CH₂Cl₂ (50 mL) and submitted to a second polycondensation reaction by following the same procedures as in the former reaction. The new product (18 g, $M_{GPC} = 7.4 \times 10^4$) was further purified by precipitation. For that purpose, heptane was added in a 1/3 volume ratio to its toluene solution (10%) in presence of a small amount of antioxidant (0.1% of Santonox-R). Once dried, the precipitate (16 g) designated as sample P(OM/

PEG200) ($M_n = 5.3 \times 10^4$, $M_w/M_n = 2.5$) was an amorphous material ($T_g = -62$ °C) of high viscosity.

The distribution of oligomers in sample PEG200 (Table I) was characterized by size exclusion chromatography (GPC) in tetrahydrofuran (THF) by using a series of three Ultrastaygel columns with upper porosity limits of 10^2 , 5×10^2 , and 10^3 Å. The values of M_{GPC} (at the peak) of the reaction products, as well as the values of M_n and M_w/M_n of sample P(OM/PEG200), were obtained by using another series of three Ultrastaygel columns having upper porosity limits of 10^3 , 10^4 , and 10^5 Å. Both series of GPC columns were calibrated with PEO and/or PEG standards.

Sodium and potassium triflates were commercial products (Alfa), while rubidium and cesium triflates were prepared by neutralization of triflic acid (Aldrich) with the corresponding hydroxides (Aldrich, 99%). These salts were purified by recrystallization in either toluene-acetonitrile (NaCF₃SO₃) or acetonitrile. All the lithium salts used in this work were prone to form hydrates when exposed to traces of humidity. Like anhydrous LiSCN,¹⁰ anhydrous LiB(Ph)₄ was obtained from etherate decomposition by heating LiB(Ph)₄·(CH₃OCH₂CH₂OCH₃)₃ (Aldrich) to 160 °C under vacuum. Before use, these salts, as well as anhydrous LiCF₃SO₃ (Aldrich, 97%) and LiClO₄ (K&K, 99.8%), were further dried at 130 °C under high vacuum. In turn, anhydrous LiN(CF₃SO₂)₂ (kindly supplied by Dr. M. Gauthier of IREQ) was heated to higher temperatures (160–170 °C). Under traces of humidity, this salt readily forms a hydrate that decomposes at 166 °C under normal pressure.

Polymer-salt mixtures were prepared under a dry atmosphere by mixing weighted quantities of 1–5% methanol solutions of each component. Solvent evaporation was carried out in ampules connected to a vacuum system. The mixtures containing the lithium salts were further dried at 130 °C for 5 h. Those containing the lithium imide were heated to 160–170 °C for an additional 1 h. The ampules were stored under a dry atmosphere in a glovebox.

DSC Measurements. Melting (or dissolution) endotherms and glass transition anomalies were recorded at heating rates of 10 and 40 °C/min, respectively. The calorimeter (Perkin-Elmer DSC-4) was flushed with dry helium. Supercooled specimens were obtained by melt quenching at a cooling rate of 320 °C/min. The values of T_g were read at the intersection of the tangent drawn through the heat capacity jump with the baseline recorded before the transition. Samples pans were filled and sealed under a dry atmosphere in the glovebox. Temperature calibrations were made by using standard materials with melting points in the range -39 to +327 °C. Energy calibrations were made by using the melting peak of indium recorded at 10 °C/min.

Conductivity Measurements. The bulk electrolytes were contained in cells consisting of two stainless steel solid cylinders encapsulated at both ends of a Teflon ring. A 1-cm diameter disk-shape electrode-electrolyte contact surface was imposed by the Teflon ring. The gap between the electrodes was 3 mm, yielding a cell constant ca. 0.4 cm⁻¹. This gap was measured at room temperature with an accuracy better than 1%, and no correction was made for the thermal expansion of the cells. The cells were filled and sealed in the glovebox. For that purpose, the bulk electrolytes were heated to 110–130 °C. The conductivity study was performed in a Model 3111 Instron temperature-controlled chamber. The temperature of the electrolytes ($30 < T < 110$ °C) was measured with an accuracy better than ± 0.5 °C by means of a digital thermometer whose probe was inserted in a well dug in the body of the cells.

The conductivity measurements were made by using the ac complex impedance technique. A complete description of this technique can be found in a recent review by Bruce.¹² In the case of blocking electrodes, it allows the separation of the bulk dc resistance of the electrolyte from the electrode-electrolyte contact impedance and from the impedances due to dielectric polarization and electrode capacitance. To apply this technique, the real part, Z' , and the imaginary part, Z'' , of the complex impedance of the cells were simultaneously recorded over the frequency range 5 Hz–13 MHz by using a Model 4192A Hewlett-Packard impedance analyzer. The impedance data were collected by means of a Model 7090A Hewlett-Packard measurement plotting system that allowed the tracing of the familiar Z'' versus Z' plot. This plot, which covers a range of decreasing frequencies,

consisted of a semicircle at high frequencies followed by an inclined spike at low frequencies. As usual,¹² the bulk dc resistance of the electrolyte was determined from the diameter of the high-frequency semicircle. The reliability of the equipment was checked against high- and low-impedance dummy cells consisting of precision resistors and capacitors.

For each electrolyte, conductivity measurements were made in duplicate (or triplicate) on distinct cells. The reproducibility was better than 5%. High-temperature data obtained with cells having a different geometry (0.5-cm-diameter electrode surface and 8-mm gap between electrodes) were superimposable on those obtained with the present cells. At 100 °C, the residual conductivity of the salt-free polymers was lower than $5 \times 10^{-8} \text{ S cm}^{-1}$.

Results and Discussion

PEO-Alkali Triflate Systems. Phase Diagrams and Thermal Properties. A few weeks after their preparation, the mixtures of PEO with lithium, sodium, or potassium triflate were all highly crystalline. No glass transition anomaly could be detected upon their first heating (from -100 °C) in the DSC apparatus. In contrast, depending on their compositions, those prepared with rubidium or cesium triflate were more or less crystalline. As will be shown shortly, a feature common to all these systems except the PEO-CsCF₃SO₃ system is the formation of a 1/1 (EO/salt) crystalline compound. In the case of the PEO-LiCF₃SO₃ system, whose phase diagram is reported in another work,¹³ this compound melts incongruently at 149 °C. It is present in all mixtures with molar ratios EO/Li < 3, where it coexists with either the salt or a second crystalline compound of 3/1 stoichiometry. In turn, this second compound, which melts congruently at 172 °C, forms a eutectic mixture with PEO. In agreement with anterior data reported on this system,¹ the eutectic composition corresponds to a molar ratio EO/Li greater than 40. This feature, together with the high rate of crystallization of the 3/1 compound,¹³ imposes a severe limitation to the temperature range of any study of the conduction properties in the concentrated, homogeneous regime. For instance, in the case of EO/Li = 16 and 8 mixtures, the last traces of crystalline compound disappear near 100 and 140 °C, respectively.

Phase diagrams of the other PEO-alkali triflate systems are depicted in Figures 1-4. It may be seen that the 1/1 compounds are the sole intermediate, crystalline phases in the case of NaCF₃SO₃, KCF₃SO₃, and RbCF₃SO₃. On the other hand, no crystalline compound forms in the case of CsCF₃SO₃. According to the calorimetric diagrams (not shown) related to these systems, the experimental stoichiometries of the crystalline compounds correspond to molar ratios EO/salt of 1.1 ± 0.1 for NaCF₃SO₃, 1.2 ± 0.1 for KCF₃SO₃, and 1.19 ± 0.05 for RbCF₃SO₃. The former two compounds melt congruently at 330 and 257 °C, respectively, while the latter melts incongruently at 193 °C. In the same order (from Na to Rb), these compounds form eutectic mixtures with PEO that melt at 54, 42, and 19 °C, respectively. The eutectic compositions are EO/salt = 12 for the PEO-NaCF₃SO₃ system and EO/salt = 9 for the other two systems.

Phase diagram of the PEO-CsCF₃SO₃ system (Figure 4) is very similar to that reported for the PEO-CsSCN system.¹⁰ Depending on the composition, the solvent-cast mixtures contain an amorphous phase that is either saturated by the salt or in equilibrium with crystalline PEO. Although T_g is invariant in either case, a small discontinuity of 3 °C occurs at the boundary between the two regions. Such a discontinuity was not observed in the case of CsSCN. The calorimetric diagram related to the PEO-CsCF₃SO₃ system is shown in Figure 5. It indicates

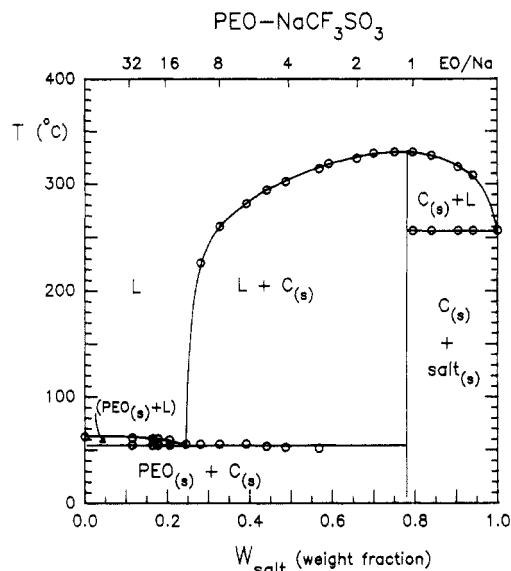


Figure 1. Phase diagram of the PEO-NaCF₃SO₃ system. The vertical boundary at $W_{\text{salt}} = 0.78$ was derived from a calorimetric analysis of the DSC data. It shows the formation of a (1.1)/1 crystalline compound designated by $C_{(s)}$. This compound forms a eutectic ($W_{\text{salt}} = 0.25$, EO/Na = 12) with PEO. It also forms a nearly monophasic eutectic ($W_{\text{salt}} \approx 1$) with the salt.

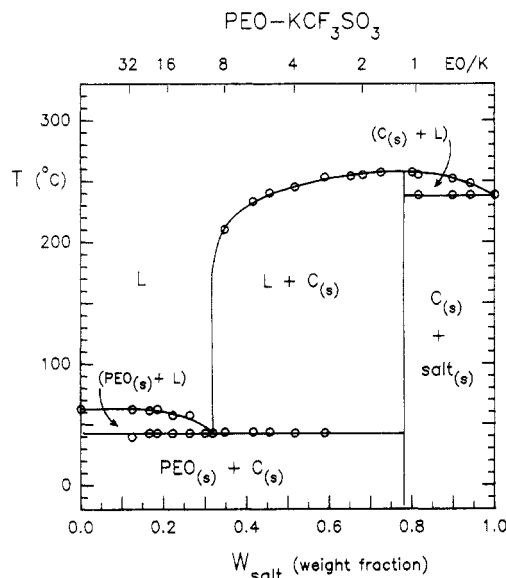


Figure 2. Phase diagram of the PEO-KCF₃SO₃ system. The vertical boundary at $W_{\text{salt}} = 0.78$ was derived from a calorimetric analysis of the DSC data. It shows the formation of a (1.2)/1 crystalline compound designated by $C_{(s)}$. This compound forms a eutectic ($W_{\text{salt}} = 0.32$, EO/K = 9) with PEO. It also forms a nearly monophasic eutectic ($W_{\text{salt}} \approx 1$) with the salt.

that at temperatures near the melting point of PEO the boundary between the two regions corresponds to a molar ratio (EO/salt = 9) identical with that reported for the PEO-CsSCN system.¹⁰

Despite these similarities concerning the PEO-CsCF₃SO₃ and PEO-CsSCN systems, an effect related to the nature of the anions is observed in the T_g composition relationships of these two systems. This effect is depicted in Figure 6, where a comparison is made on a molar basis of the T_g data of melt-quenched specimens. These data correspond to mixtures in which all the polymer is dissolved in the amorphous phase. It may be seen that prior to saturation the T_g elevation produced by CsCF₃SO₃ is lower than that produced by CsSCN. The departure is maximum near the midpoint between salt-free PEO and saturation. This feature appears to be cation size inde-

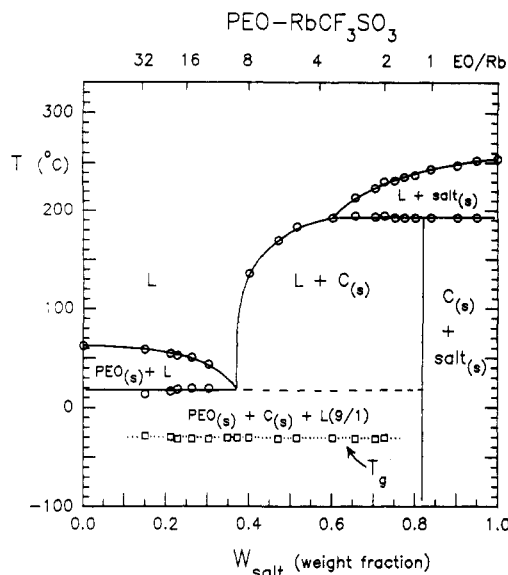


Figure 3. Phase diagram of the PEO-RbCF₃SO₃ system. The vertical boundary at $W_{\text{salt}} = 0.82$ was derived from a calorimetric analysis of the DSC data. It shows the formation of a (1.2)/1 crystalline compound designated by $C_{(s)}$. This compound forms a eutectic ($W_{\text{salt}} = 0.37$, EO/Rb = 9) with PEO. The eutectic mixture was partly crystallized (or supercooled) as indicated by the T_g tie line at -31 °C.

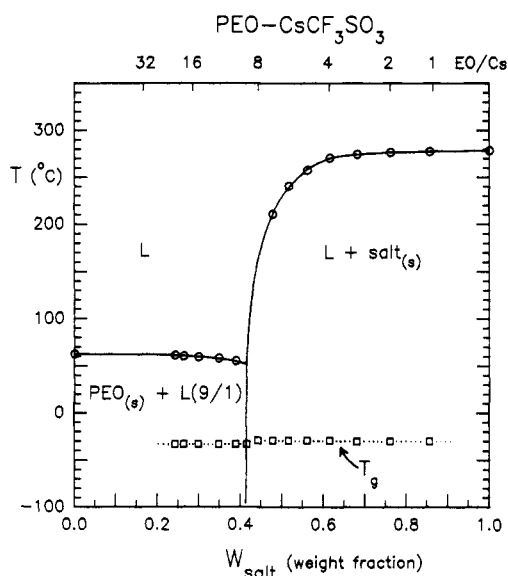


Figure 4. Phase diagram of the PEO-CsCF₃SO₃ system. At low temperatures, each mixture consists of an amorphous phase that is either in equilibrium with crystalline PEO ($T_g = -33$ °C) or saturated by the salt ($T_g = -30$ °C). The vertical segment at $W_{\text{salt}} = 0.415$ (EO/Cs = 9), which corresponds to the boundary between these two regions, was derived from the calorimetric diagram shown in Figure 5.

pendent since, as shown in Figure 7, it also applies to a similar comparison made for the PEO-LiCF₃SO₃ and PEO-LiSCN systems. Note that on a molar basis saturation occurs at considerably higher salt contents in these latter systems (EO/Li = 2.7 for LiCF₃SO₃ and 3.0 for LiSCN). Due to the high rate of crystallization of the 1/1 compounds in the mixtures of the other systems, their T_g -composition relationships could not be constructed up to saturation. In those cases, melt-quenching yielded supercooled mixtures for salt contents inferior to the eutectic compositions only. Nevertheless, the same effect as that depicted in Figures 6 and 7 was apparent over this partial range of compositions.

According to the features of the phase diagrams depicted in Figures 2-4, PEO electrolytes containing KCF₃SO₃,

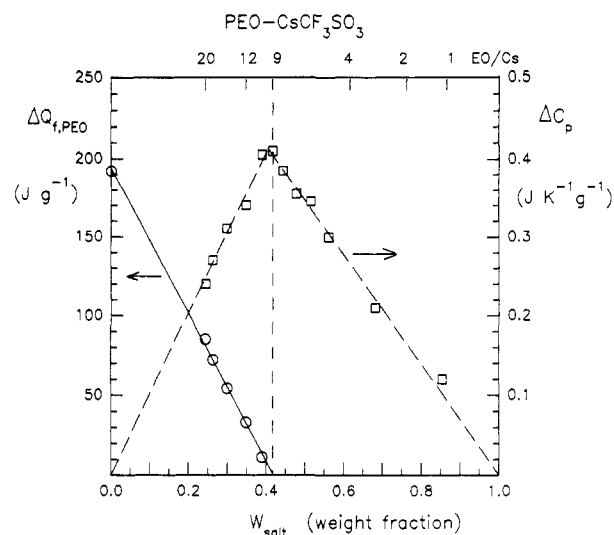


Figure 5. Calorimetric diagram related to the thermal events recorded at low temperatures on the as-cast mixtures of the PEO-CsCF₃SO₃ system. This diagram shows plots as a function of the salt content of both the heat capacity increase at T_g per gram of sample, ΔC_p , and the heat of fusion of the PEO moiety per gram of sample, $\Delta Q_{f,PEO}$. From these plots, it may be inferred that the composition of the amorphous phase ($W_{\text{salt}} = 0.415$, EO/Cs = 9) is temperature independent over the range from -30 to $+60$ °C.

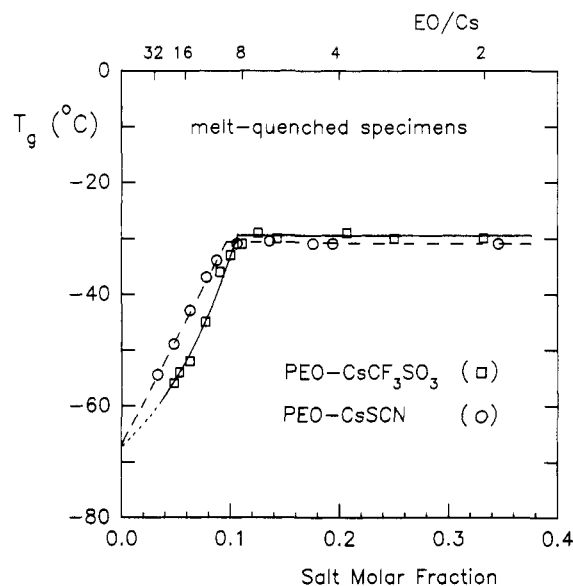


Figure 6. Comparison of the T_g -composition relationships obtained for supercooled mixtures of the PEO-CsCF₃SO₃ and PEO-CsSCN systems.

RbCF₃SO₃, or CsCF₃SO₃ in a molar ratio EO/M = 9 ($c = 1.5$ – 1.7 mol/kg) are totally amorphous at moderate temperatures. Since such concentrated, PEO amorphous electrolytes cannot be obtained with either NaCF₃SO₃ or LiCF₃SO₃, attempts were made to prepare comparable electrolytes with copolymer P(OM/PEG200) described in the Experimental Section. This copolymer is an oxy-methylene-linked PEO sample having a higher molecular weight ($M_n = 5.3 \times 10^4$) than the PEO sample used in this study ($M_n = 3.9 \times 10^3$). In its salt-free form, the P(OM/PEG200) sample was an amorphous material that did not exhibit any crystallization under cooling at 5 °C/min in the DSC apparatus. As shown in Figure 8, where a comparison is made of DSC curves recorded on mixtures of LiCF₃SO₃ in a molar ratio O/Li = 9 (O = oxygen atom) with this copolymer and with PEO, there is no evidence for crystallization of the 3/1 compound in the former mixture.

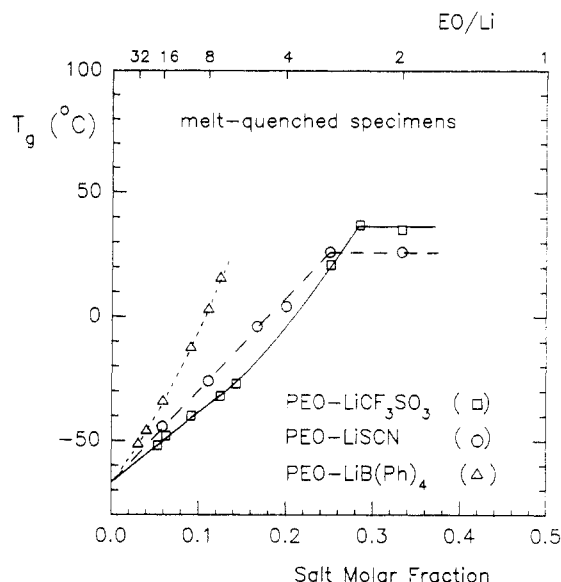


Figure 7. Comparison of the T_g -composition relationships obtained for supercooled mixtures of the PEO-LiCF₃SO₃, PEO-LiSCN, and PEO-LiB(Ph)₄ systems. Phase diagram of the PEO-LiB(Ph)₄ system is shown in Figure 12.

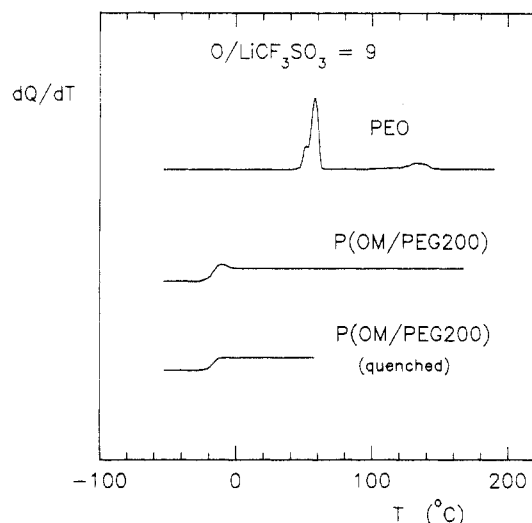


Figure 8. Comparison of DSC heating curves recorded at 40 °C/min on LiCF₃SO₃ mixtures in a molar ratio O/Li = 9 with PEO and copolymer P(OM/PEG200).

Unfortunately, this feature does not apply to comparable mixtures prepared with NaCF₃SO₃ and KCF₃SO₃ (RbCF₃SO₃ was not examined). As depicted in Figure 9 for NaCF₃SO₃, compound crystallization in sample P(OM/PEG200) is revealed by both an endotherm at 233 °C and an increase in T_g (from -33 to -20 °C) after melt-quenching from 270 °C. A similar behavior was observed for KCF₃SO₃, though the endotherm was recorded at 210 °C. Since the mixture of the same composition with PEO is a eutectic mixture that melts at 42 °C, this feature suggests that the liquidus curve of the 1/1 compound was shifted to lower salt contents than in the case of the PEO-KCF₃SO₃ system (Figure 2). Further studies made with CsCF₃SO₃ provided evidence for a thermodynamical instability related to the presence of the oxymethylene units in the copolymer. Partial salt precipitation occurred near 100–130 °C on the first heating of the O/M = 9 mixture. As inferred from the T_g depression of 10 °C measured after quenching from 150 °C, the composition of the polymeric phase in this mixture was changed to a molar ratio O/M = 11.

Beside these particularities of the phase behavior of the O/M = 9 electrolytes prepared with sample P(OM/

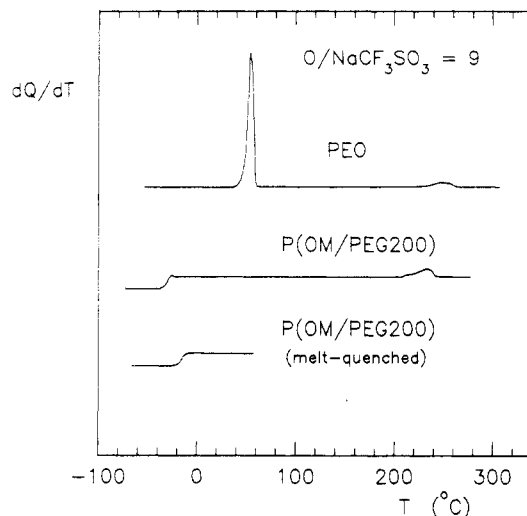


Figure 9. Comparison of DSC heating curves recorded at 40 °C/min on NaCF₃SO₃ mixtures in a molar ratio O/Na = 9 with PEO and copolymer P(OM/PEG200).

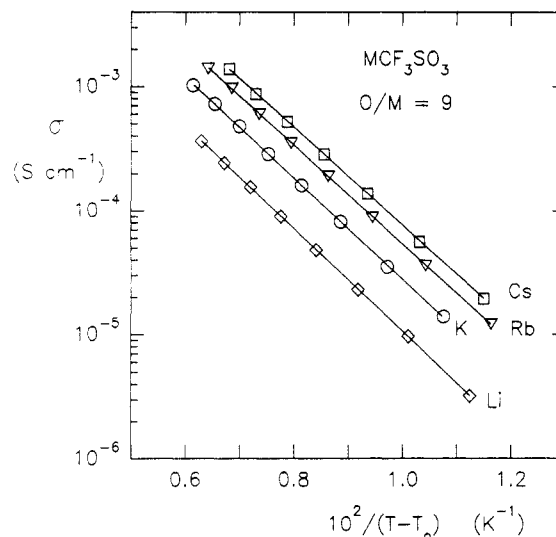


Figure 10. Best fits of eq 1 to the conductivity data of P(OM/PEG200)-LiCF₃SO₃ and PEO-MCF₃SO₃ (M = K, Rb, and Cs) amorphous electrolytes having a molar ratio O/M = 9. The values of T_0 of these electrolytes are listed in Table II together with the values of parameters A , and B of the fits.

PEG200), another point concerns the chemical stability of this copolymer in presence of traces of strong acid. GPC characterizations made at different intervals on these various electrolytes showed a progressive depolymerization of the materials containing NaCF₃SO₃ and CsCF₃SO₃. After 6 months of storage, their values of M_n were lowered to 330 ($M_w/M_n = 1.3$) and 3600 ($M_w/M_n = 1.7$), respectively. On the other hand, those of the materials containing LiCF₃SO₃ and KCF₃SO₃ were almost unchanged. This effect was probably due to the presence of traces of triflic acid in the former two salts. To clarify this point, mixtures with triflic acid were prepared in a molar ratio O/acid = 200 with both salt-free P(OM/PEG200) and salt-free PEO. After a few days, the GPC curves recorded on the mixture prepared with the copolymer showed a quantitative depolymerization, while those of the control made with PEO were unchanged.

Conductivity Behavior. Figure 10 shows fits of eq 1 to the conductivity data of the O/M = 9 electrolytes prepared with LiCF₃SO₃ in copolymer P(OM/PEG200), on the one hand, and KCF₃SO₃, RbCF₃SO₃, and CsCF₃SO₃ in PEO, on the other hand. The data cover the range 30 < T < 100 °C where the four electrolytes were homogeneous, non-

Table II
Values of T_g and Parameters T_0 , A , and B of the Best Fits of Eq 1 to the Conductivity Data of the P(OM/PEG200) and PEO Electrolytes Containing Various Alkali Triflates in a Molar Ratio O/M = 9

sample	T_g (°C)	T_0 (°C)	A (S cm ⁻¹)	B (K)	$T_g - T_0$ (°C)
P(OM/PEG200)-LiCF ₃ SO ₃	-21	-59	0.149	956	38
PEO-KCF ₃ SO ₃	-36	-63	0.334	941	27
PEO-RbCF ₃ SO ₃	-31	-56	0.506	916	25
PEO-CsCF ₃ SO ₃	-33	-57	0.687	915	24

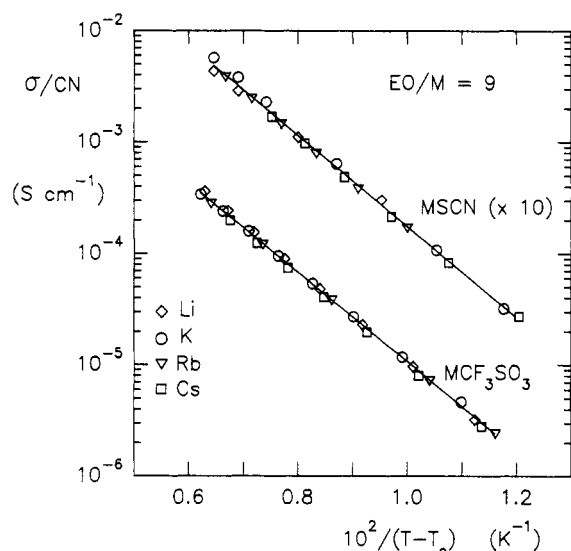


Figure 11. Semilogarithmic plots of σ/CN as a function of $(T - T_0)^{-1}$ for the MCF₃SO₃ electrolytes described in Table II and for comparable PEO amorphous electrolytes ($T_g = -30 \pm 1$ °C) containing MSCN in a molar ratio EO/M = 9. In these plots, CN is the apparent coordination number of the cation (1 for Li⁺, 3 for K⁺, 5 for Rb⁺, and 7 for Cs⁺). Parameter T_0 is adjusted to $(T_g - 25)$ °C for all the PEO electrolytes and to $(T_g - 38)$ °C for the P(OM/PEG200)-LiCF₃SO₃ electrolyte. For clarity, the data of the PEO-MSCN electrolytes are shifted by a factor of 10 along the vertical axis.

crystalline materials. Once melted at 42 °C, the mixture containing KCF₃SO₃ remained completely amorphous upon its cooling to 30 °C. The T_g 's of these electrolytes are listed in Table II with the values of the parameters T_0 , A , and B of the best fits to the data. As in the former work on the alkali thiocyanates,¹⁰ the parameters T_0 of the PEO electrolytes correspond to $(T_g - 25)$ °C, approximately. That of the P(OM/PEG200) electrolyte, which roughly coincides with the other values of T_0 in Table II, corresponds to $(T_g - 38)$ °C. This departure may result from the difference in the nature (or the molecular weight) of the polymers.

In the former work on the alkali thiocyanates,¹⁰ solubility data at low and moderate temperatures were interpreted in terms of a chemical model for cation solvation. The reliability of this model was reinforced by more convincing arguments based on the solubility behavior of the same salts in atactic poly(methyl glycidyl ether).¹⁴ According to this model, the apparent coordination numbers (CN) of the alkali cations in amorphous PEO increase in the same ratio as the cation surface. When given in terms of EO units per cation, the values of CN are about^{10,14} 1 for Li⁺, 2 for Na⁺, 3 for K⁺, 5 for Rb⁺, and 7 for Cs⁺. Figure 11 shows plots of $\log(\sigma/CN)$ as a function of $1/(T - T_0)$ for both the present electrolytes and comparable electrolytes prepared in the same molar ratio with the corresponding alkali thiocyanates. The latter electrolytes exhibited T_g values of -30 ± 1 °C. All the data except those related to LiCF₃SO₃ in P(OM/PEG200) are com-

pared on a $T - T_0$ scale in which T_0 corresponds to $(T_g - 25)$ °C. The value of T_0 for the P(OM/PEG200) electrolyte is that listed in Table II. It may be seen that each series of salts with a common anion yields a single curve indicating that σ increases in the same ratio as CN. For clarity, the composite curve related to the thiocyanates has been shifted by a factor of 10 along the vertical axis. Its actual magnitude is greater by a factor of 1.6 than that of the triflates.

Since CN was proven to increase in the same ratio as the cation surface,^{10,14} the invariance of σ/CN with cation size indicates that ion mobility decreases linearly with increasing cation charge density. This feature, which reveals a coupling between the dynamics of the ions of opposite charge, was previously attributed to the effect of the cation-oxygen binding energy on the ion motion.¹⁰ In this speculative, preliminary interpretation, each electrolyte was assumed to consist of free ions in a latticelike arrangement. Furthermore, because the electrolytes had the same salt content (i.e., same average distance between the ions), the ion-ion interactions accounting for the coupling were assumed to be independent of the cation size. But, by analogy with the molten salt mixtures,⁷ it is likely that anion polarization may also contribute to the correlation between conductivity and cation charge density. Like cation-oxygen binding energy, interaction energy related to anion polarization should increase with cation charge density. The molar polarizability of SCN⁻ was reported¹⁵ to be 6.4×10^{-3} nm³. In comparison, the molar polarizabilities of the alkali cations^{16,17} increase from about 3×10^{-5} nm³ for Li⁺ to $(2.2-2.9) \times 10^{-3}$ nm³ for Cs⁺. On this ground, it is conceivable that SCN⁻, which is classified as a soft anion,¹ can undergo sizable polarization under an asymmetric, cationic environment. Unfortunately, no data could be found in the literature concerning the polarizability (or softness) of CF₃SO₃⁻.

PEO Electrolytes with Lithium Salts of Different Polarizabilities. Among the anions less polarizable than SCN⁻ there is ClO₄⁻. This anion, which is classified as a hard anion,¹ has a reported polarizability¹⁸ of 4.2×10^{-3} nm³. On the other hand, its ionic radius ($r_i = 0.236$ nm) is slightly greater than that of SCN⁻ ($r_i = 0.195-0.213$ nm).¹ Note that ions of this size are among the smallest anions that yield alkali salts soluble in PEO. Below this limit, salt lattice energy is no longer favorable to dissolution. At the other extreme, B(Ph)₄⁻ ($r_i = 0.421$ nm), which is classified¹ as a softer anion than SCN⁻, is among the largest symmetrical, inorganic anions that yield alkali salts soluble in PEO.

The phase diagram of the PEO-LiB(Ph)₄ system is depicted in Figure 12. On a molar basis, solubility of LiB(Ph)₄ in PEO is lower than those of LiSCN and LiClO₄. For instance, at 190 °C it corresponds to a molar ratio EO/Li ca. 6.5 compared to 1.5 for LiSCN and to 1 for LiClO₄.¹³ Another feature of LiB(Ph)₄ is the high melting point (170 °C) of its 5.5/1 compound with PEO. In comparison, the 6/1 compound with LiClO₄ melts at 63 °C.¹³ On the other hand, PEO-LiSCN mixtures with EO/Li > 4 are either noncrystallizable or exhibit melting points inferior to that of salt-free PEO.¹⁰ In view of these features, electrolytes with these three salts were examined in the same molar ratio (EO/Li = 11) as the eutectic composition of the PEO-LiB(Ph)₄ system.

A fourth salt is included in the present comparison. This salt is the lithium imide LiN(CF₃SO₂)₂ that was recently reported by Armand et al.¹⁸ as yielding PEO amorphous electrolytes of low T_g over a wide range of compositions in the concentrated regime. As pointed out by these

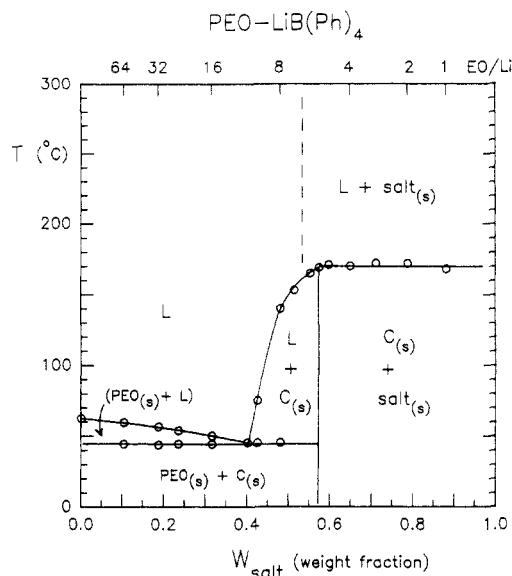


Figure 12. Phase diagram of the PEO-LiB(Ph)₄ system. The vertical boundary at $W_{\text{salt}} = 0.57$ was derived from a calorimetric analysis of the DSC data. It shows the formation of a (5.5)/1 crystalline compound designated by $C_{(s)}$. This compound forms a eutectic ($W_{\text{salt}} = 0.40$, EO/Li = 11) with PEO and exhibits an incongruent melting at 170 °C. Over the range 170–300 °C, salt was absent for EO/Li = 7 but present for EO/Li = 6. Thus, the dashed line at $W_{\text{salt}} = 0.53$ (EO/Li = 6.5) may be considered as a good approximation of the salt liquidus curve.

authors, the other interesting features of the anion $N(\text{CF}_3\text{SO}_2)_2^-$ are both its great charge delocalization and its large electronegativity.¹⁸ In that respect, this anion is similar to ClO_4^- and should be classified as a hard anion. Comparative studies were previously reported on the conductivity magnitudes of $\text{LiN}(\text{CF}_3\text{SO}_2)_2$ and LiClO_4 in concentrated electrolytes made with either PEO¹³ or aprotic solvents having greater dielectric constants than PEO.⁴ In either case, the data were slightly favorable to the former salt. As reported in the study related to PEO,¹³ the T_g -composition relationship of LiClO_4 is much steeper than that of the lithium imide. This feature will be considered in the present comparison. Like LiClO_4 , $\text{LiN}(\text{CF}_3\text{SO}_2)_2$ forms a 6/1 compound with PEO.¹³ This compound, which melts at 46 °C, does not crystallize in mixtures having molar ratios EO/Li greater than 6.

Figure 13 shows fits of eq 1 to the conductivity data of the EO/Li = 11 electrolytes prepared with the four salts. As in the former fits, parameter T_0 is adjusted to $(T_g - 25)$ °C. The values of T_g are -43 °C for $\text{LiN}(\text{CF}_3\text{SO}_2)_2$, -36 °C for LiSCN , -32 °C for LiClO_4 , and -17 °C for $\text{LiB}(\text{Ph})_4$. Thus, contrary to the anion $N(\text{CF}_3\text{SO}_2)_2^-$, the anion $\text{B}(\text{Ph})_4^-$ has a detrimental effect on the segmental motion in PEO electrolytes (T_g data for other concentrations of $\text{LiB}(\text{Ph})_4$ are depicted in Figure 7). Inspection of Figure 13 shows that for a given value of $T - T_0$ (or $T - T_g$), the conductivities of $\text{LiB}(\text{Ph})_4$, LiSCN , and LiClO_4 increase with decreasing polarizability of the corresponding anions. In turn, in this comparison made on the basis of a corresponding state of thermal energy, conductivity of $\text{LiN}(\text{CF}_3\text{SO}_2)_2$ remains slightly greater than that of LiClO_4 .

According to the data in Figure 11, reduced conductivity of LiCF_3SO_3 in PEO would be inferior by a factor of 1.6 to that of LiSCN . On this basis, reduced conductivity of the lithium imide would be greater by a factor of 6 than that of LiCF_3SO_3 . Conductivity data of these two salts were compared by Webber⁴ in aprotic solvents having dielectric constants (ϵ) of 13 and 36, respectively. The salt concentration was 1 mol/L, and the solvents were

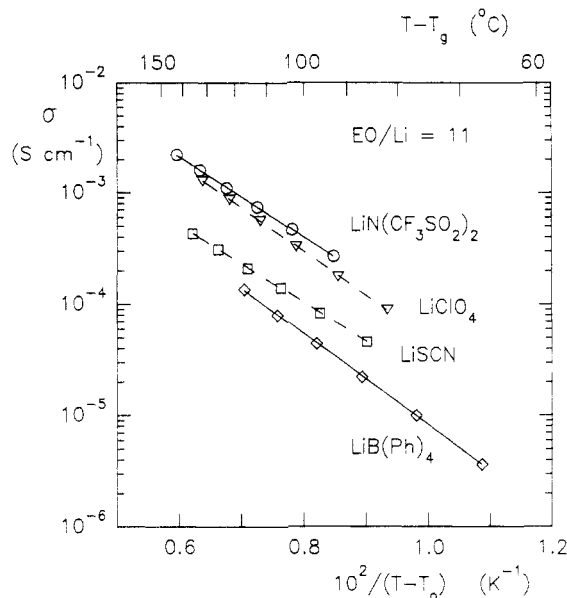


Figure 13. Conductivity data of PEO amorphous electrolytes containing $\text{LiB}(\text{Ph})_4$, LiSCN , LiClO_4 , and $\text{LiN}(\text{CF}_3\text{SO}_2)_2$ in a molar ratio EO/Li = 11. Plots made according to eq 1 with T_0 adjusted to $(T_g - 25)$ °C. Values of T_g are -17 °C for $\text{LiB}(\text{Ph})_4$, -36 °C for LiSCN , -32 °C for LiClO_4 , and -43 °C for $\text{LiN}(\text{CF}_3\text{SO}_2)_2$.

mixtures of propylene carbonate with different amounts of ether(s) (1,3-dioxolane and 1,2-dimethoxyethane). In the former solvent ($\epsilon = 13$), the Walden product $\sigma\eta$ (η = viscosity) related to $\text{LiN}(\text{CF}_3\text{SO}_2)_2$ was greater by a factor of 5 than that of LiCF_3SO_3 . In the second solvent ($\epsilon = 36$), this factor was lowered to 2.4. This change, together with the greater Walden products (by a factor of 2–3) of both salts in the latter solvent, was interpreted as an indication that ion pairing took place to a lesser extent in the $\text{LiN}(\text{CF}_3\text{SO}_2)_2$ electrolytes than in the LiCF_3SO_3 electrolytes. A comparison was also made by Webber⁴ of five other lithium salts (LiBF_4 , LiClO_4 , LiAsF_6 , LiPF_6 , and a cyclic imide) in the solvent with $\epsilon = 36$. The Walden product of LiClO_4 was reported to be about the same as that of $\text{LiN}(\text{CF}_3\text{SO}_2)_2$ (and the cyclic imide). That of LiBF_4 was 40% lower, while those of LiAsF_6 and LiPF_6 were 20% higher. Thus, the greater dielectric constant of this solvent with respect to PEO ($\epsilon = 5$ at 65 °C)¹⁹ appears to have little effect on the conductivity magnitude of LiClO_4 relative to that of the lithium imide.

As compiled a few years ago by Salomon,²⁰ the constants of formation of ion pairs at infinite dilution (K_p°) related to $\text{LiB}(\text{Ph})_4$, LiAsF_6 , and LiClO_4 in THF ($\epsilon = 7.36$)²¹ are 1.26×10^4 , 2.76×10^5 , and 4.84×10^7 L/mol, respectively. Those of $\text{LiB}(\text{Ph})_4$, LiAsF_6 , and LiBF_4 in 2-methyltetrahydrofuran ($\epsilon = 6.24$)²¹ are 8.33×10^4 , 2.02×10^7 , and 9.5×10^9 L/mol, respectively. These data indicate that, in the absence of long-range Coulombic interactions, $\text{LiB}(\text{Ph})_4$ is considerably more dissociated than either LiClO_4 or LiAsF_6 . This feature is just the opposite of what could be deduced from the data in Figure 13 if ion pairing accounted for the difference between conductivity of $\text{LiB}(\text{Ph})_4$ and LiClO_4 in PEO.

Recently, Petrucci and Eyring²¹ reported a critical analysis of molar conductivity of LiClO_4 and LiAsF_6 at low concentrations in various aprotic solvents including ethers having dielectric constants ($\epsilon = 6$ –7) comparable to that of PEO. In this analysis, the decrease with increasing concentration of the stoichiometric values of K_p deduced from the conductivity data was rationalized in terms of physical, many-body interactions only. Computations of

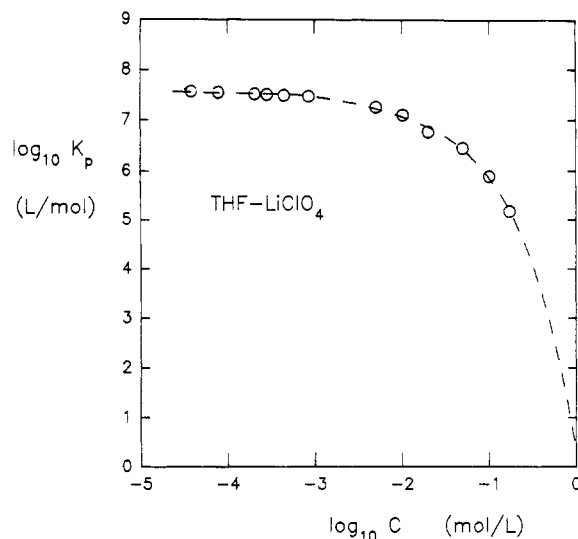


Figure 14. Bilogarithmic plot of K_p , the stoichiometric equilibrium constant for ion pair formation in THF- LiClO_4 electrolytes at 25 °C, as a function of LiClO_4 concentration. Data reported by Petrucci and Eyring.²¹ The dashed curve depicts a tentative extrapolation of the experimental data to a concentration of 1 mol/L.

K_p based on a model that took into account the effect of these interactions on the activity coefficients of the ion pairs and the free ions were shown to fit the experimental data. This model, which deliberately ignored the formation of triple ions as specific conducting species, also could account for the minimum observed in the concentration dependence of the molar conductivity of the various systems. According to this model, above a critical concentration that depends on the nature of the salt and the dielectric constant of the solvent, the degree of dissociation of the ion pairs increases with increasing concentration. For instance, in the case of the THF- LiClO_4 system, this critical concentration is as low as 3×10^{-2} mol/L. As shown in Figure 14, the values of K_p reported for this system decrease markedly with increasing concentration. A tentative extrapolation of the data to a concentration of 1 mol/L yields a value of K_p of 2 L/mol that corresponds to a degree of dissociation of 50%.

At low concentrations, the conductivity behavior of polyether electrolytes is very similar to that of aprotic solvent electrolytes. Recently, Gray²² reported the concentration dependence of molar conductivity of LiClO_4 in a P(OM/PEG) copolymer over the concentration range 3×10^{-4} to 1.2 mol/L. At 25 °C, molar conductivity of this system exhibits a minimum at a concentration ca. 1×10^{-2} mol/L comparable to that of the THF- LiClO_4 system. For the concentrations below 0.1 mol/L, the data could be rationalized in terms of a classical equation that accounts for the formation of triple ions. Although no values of the constants of formation of ion pairs (K_p) and triple ions (K_T) were reported, Gray mentioned that over this range the salt was mostly present as ion pairs with some triple ion formation.

The model of Petrucci and Eyring,²¹ which suggests an extensive dissociation of ion pairs at high concentration (see Figure 14), agrees with most of the features reported on concentrated polyether electrolytes. Among these features, there is the correlation already quoted^{8,9} between the self-diffusion coefficients of the ions and the conductivity magnitude at moderate temperatures. There is also the superimposition of the plots shown in Figure 11 that indicates that cation size has essentially no effect on the temperature dependence of conductivity. As mentioned in a former work,¹⁰ this feature shows the absence of any

effect that could be related to a change in the temperature coefficient of K_p (or K_T) with cation charge density.

Evidence for an extensive dissociation of ion pairs is also found in the Raman spectra (anion vibration) reported by Torell and Schantz^{23,24} for poly(propylene oxide) (PPO) electrolytes containing LiClO_4 and NaCF_3SO_3 in various molar ratios over the range $O/M = 5$ –1000. However, the high degrees of dissociation (87% for LiClO_4 and 50% for NaCF_3SO_3)²⁴ deduced from these spectra were reported to remain constant over the concentration range 0.02–1 mol/L (i.e., from $O/M = 1000$ to 16). Since the lower limit of this range is near the concentration where a minimum occurs in the concentration dependence of the molar conductivity of comparable systems,²² this feature may cast some doubts on the reliability of the band assignments.^{25,26} As suggested by Gray,²⁵ it is possible that the band assigned to the ion pairs, which increases in relative intensity only for concentrations greater than 1 mol/L, corresponds to free anions in a latticelike environment. If that is the case, the intensification of this band, which is more marked for NaCF_3SO_3 than for LiClO_4 , might result from anion polarization.

Conclusion

The presence of the many-body interactions in concentrated PEO electrolytes not only contributes to a substantial reduction of ion pairing but also leads to a situation where factors other than ion pairing become dominant in the conduction process. According to the present data, short-range polar effects such as ion-dipole interactions and anion polarization appear to play a nonnegligible part among these factors. The problem, however, is to separate the contributions of these effects from each other and from those associated with long- and short-range Coulombic interactions. Although there is no direct approach to tackle this problem, the present study reveals interesting features that may help to orient further works to clarify the correlation between the cation size and conductivity of alkali thiocyanates and triflates. Since anion polarization appears to reduce the conductivity of LiB(Ph)_4 and LiSCN with respect to that of LiClO_4 , there are good reasons to consider that this effect may take a part of this correlation. Although the polarizabilities of CF_3SO_3^- and $\text{N(CF}_3\text{SO}_2)_2^-$ remain to be determined, it is likely that the same effect accounts for the difference in the conductivity of LiCF_3SO_3 and $\text{LiN(CF}_3\text{SO}_2)_2$. If so, PEO electrolytes containing alkali salts with a common anion such as ClO_4^- or $\text{N(CF}_3\text{SO}_2)_2^-$ would exhibit conductivity magnitudes less sensitive to the cation size than the present electrolytes.

Acknowledgment. This work was supported by the Research Institute of Hydro-Quebec (IREQ) and the Natural Sciences and Engineering Research Council of Canada. We thank Dr. Michel Gauthier of IREQ for supplying the lithium imide and for helpful discussions.

References and Notes

- Gray, F. M. *Solid Polymer Electrolytes*; VCH Publishers: New York, 1991.
- Gauthier, M.; Armand, M.; Muller, D. In *Electroresponsive Molecular and Polymeric Systems*; Skotheim, T. A., Ed.; Marcel Dekker Inc.: New York, 1988; Vol. 1, p 41.
- Barthel, J.; Gores, H. J.; Schmeer, G.; Wachter, R. In *Topics in Current Chemistry*; Boschke, F. L., Ed.; Springer-Verlag: New York, 1983; Vol. 111, p 33.
- Webber, A. J. *Electrochem. Soc.* 1991, 138, 2586.
- Armand, M. B.; Chabagno, J. M.; Duclot, M. J. In *Fast Ion Transport in Solids*; Vashishta, P.; Mundy, J. N.; Shenoy, G. K., Eds.; Elsevier North Holland: New York, 1979; p 131.

- (6) Angell, C. A. *J. Phys. Chem.* **1964**, *68*, 1917.
- (7) Moynihan, C. T. In *Ionic Interactions from Dilute Solutions to Fused Salts*; Petrucci, S., Ed.; Academic Press: New York, 1971; Vol. I, p 261.
- (8) Boden, N.; Leng, S. A.; Ward, I. M. *Solid States Ionics* **1991**, *45*, 261.
- (9) Al-Mударis, A. A.; Chadwick, A. V. *Br. Polym. J.* **1988**, *20*, 213.
- (10) Besner, S.; Prud'homme, J. *Macromolecules* **1989**, *22*, 3029.
- (11) Booth, C.; Nicholas, C. V.; Wilson, D. J. In *Polymer Electrolyte Reviews*; MacCallum, J. R., Vincent, C. A., Eds.; Elsevier Applied Science: New York, 1989; Vol. 2, p 229.
- (12) Bruce, P. G. In *Polymer Electrolyte Reviews*; MacCallum, J. R., Vincent, C. A., Eds.; Elsevier Applied Science: New York, 1987; Vol. 1, p 237.
- (13) Vallée, A.; Besner, S.; Prud'homme, J. *Electrochim. Acta* **1992**, *37*, 1579.
- (14) Dumont, M.; Boils, D.; Harvey, P. E.; Prud'homme, J. *Macromolecules* **1991**, *24*, 1791.
- (15) Jindal, H. R.; Harrington, G. W. *J. Phys. Chem.* **1967**, *71*, 1688.
- (16) Böttcher, C. J. F. *Recl. Trav. Chim. Pays Bas* **1946**, *65*, 19.
- (17) Kumar, M.; Shanker, J. *J. Chem. Phys.* **1992**, *96*, 5289.
- (18) Armand, M.; Gorecki, W.; Andréani, R. In *Second International Symposium on Polymer Electrolytes*; Scrosati, B., Ed.; Elsevier Applied Science: New York, 1990; p 91.
- (19) Gray, F. M.; Vincent, C. A.; Kent, M. *J. Polym. Sci., Polym. Phys. Ed.* **1989**, *27*, 2011.
- (20) Salomon, M. *Electrochim. Acta* **1985**, *30*, 1021.
- (21) Petrucci, S.; Eyring, E. M. *J. Phys. Chem.* **1991**, *95*, 1731.
- (22) Gray, F. M. *Solid State Ionics* **1990**, *40/41*, 637.
- (23) Torell, L. M.; Schantz, S. In *Polymer Electrolyte Reviews*; MacCallum, J. R., Vincent, C. A., Eds.; Elsevier Applied Science: New York, 1989; Vol. 2, p 1.
- (24) Schantz, S. *J. Chem. Phys.* **1991**, *94*, 6296.
- (25) Gray, F. M. *J. Polym. Sci., Polym. Phys. Ed.* **1991**, *29*, 1441.
- (26) Another explanation of this feature may be found in the phase behavior of these systems. According to a recent study made in our laboratory (Vachon, C.; Prud'homme, J., unpublished results), solutions of LiClO₄ in PPO exhibit a microphase separation below a critical concentration that corresponds to a ratio O/Li = 10. More dilute mixtures of this system consist of microdomains of a fixed composition (O/Li = 10) in equilibrium with salt-free PPO. These microdomains are stabilized by the ion-ion interactions.